THE JOURNAL OF BIOLOGICAL CHEMISTRY VOL. 280, NO. 47, pp. 39403–39416, November 25, 2005

Nitric Oxide Induces TIMP-1 Expression by Activating the Transforming Growth Factor β-Smad Signaling Pathway*

Received for publication, April 15, 2005, and in revised form, September 12, 2005 Published, JBC Papers in Press, September 23, 2005, DOI 10.1074/jbc.M504140200

El-Sayed Akool[1,2], Anke Doller[1], Roswitha Müller, Paul Gutwein, Cuiyan Xin, Andrea Huwiler, Josef Pfeilschifter, and Wolfgang Eberhardt[3]

From the Pharmazentrum Frankfurt/ZAFES, Klinikum der Johann Wolfgang Goethe-Universität, D-60590 Frankfurt am Main, Germany

Excessive accumulation of the extracellular matrix is a hallmark of many inflammatory and fibrotic diseases, including those of the kidney. This study addresses the question whether NO, in addition to inhibiting the expression of MMP-9, a prominent metalloprotease expressed by mesangial cells, additionally modulates expression of its endogenous inhibitor TIMP-1. We demonstrate that exogenous NO has no modulatory effect on the extracellular TIMP-1 content but strongly amplifies the early increase in cytokine-induced TIMP-1 mRNA and protein levels. We examined whether transforming growth factor β (TGFβ), a potent profibrotic cytokine, is involved in the regulation of NO-dependent TIMP-1 expression. Experiments utilizing a pan-specific neutralizing TGFβ antibody demonstrate that the NO-induced amplification of TIMP-1 is mediated by extracellular TGFβ. Mechanistically, NO causes a rapid increase in Smad-2 phosphorylation, which is abrogated by the addition of neutralizing TGFβ antisera. Similarly, the NO-dependent increase in Smad-2 phosphorylation is prevented in the presence of an inhibitor of TGFβ-RI kinase, indicating that the NO-dependent activation of Smad-2 occurs via the TGFβ-type I receptor. Furthermore, activation of the Smad signaling cascade by NO is corroborated by the NO-dependent increase in nuclear Smad-4 level and is paralleled by increased DNA binding of Smad-2/3 containing complexes to a TIMP-1-specific Smad-binding element (SBE). Reporter gene assays revealed that NO activates a 0.6-kb *TIMP-1* gene promoter fragment as well as a TGFβ-inducible and SBE-driven control promoter. Chromatin immunoprecipitation analysis also demonstrated DNA binding activity of Smad-3 and Smad-4 proteins to the TIMP-1-specific SBE. Finally, by enzyme-linked immunosorbent assay, we demonstrated that NO causes a rapid increase in TGFβ$_1$ levels in cell supernatants. Together, these experiments demonstrate that NO by induction of the Smad signaling pathway modulates TIMP-1 expression.

A number of pathological conditions characterized by excessive deposition of extracellular matrix (ECM)[4] are most commonly due to failures in the coordinate expression of proteins regulating collagen metabolism. Most prominently, these include members of the family of matrix metalloproteinases (MMPs) and their intrinsic inhibitors, the tissue inhibitors of MMPs (TIMPs) (for review see Refs. 1 and 2). In particular, an imbalance between MMPs and TIMPs is thought to be a main cause of increased matrix deposition, consequently resulting in tissue fibrosis within different organs, including lung, liver, heart, and kidney. The regulation of MMP-9 (gelatinase B), one of the MMPs crucially involved in the progression of renal fibrosis, occurs, as is the case for most MMPs, at different levels, including transcription, activation of the latent proenzyme by endogenous MMP activators, and finally by inhibition of the enzyme activity by the intrinsic MMP-9 inhibitor TIMP-1. TIMP-1 expression in most cell types is low but is transcriptionally induced by a variety of agents, including serum, growth factors, phorbol esters, and proinflammatory cytokines (3–5).

Within the kidney, the glomerular mesangial cells (MC) are thought to be a main cellular source of renal MMP-9 and TIMP-1 synthesis, and the expression of both proteins is highly induced by proinflammatory cytokines (5). In addition, MC are able to respond to a variety of other biological mediators, including eicosanoids, growth factors, reactive oxygen species, and NO, the latter one being one of the most versatile products of the activated MC (6–8). In renal MC, NO can modulate the expression of several ECM degrading proteases and intrinsic inhibitors, including MMP-9 (5), MMP-13 (9), tissue plasminogen activator (10), plasminogen activator inhibitor-1 (10), and TIMP-1 (5). The modulatory effects of NO on the expression pattern of cytokine-inducible genes that contribute to ECM homeostasis are considered to be a critical step in the initiation and propagation of fibrotic processes within the kidney (11–13). The mechanisms by which NO can influence MMP activity are quite complex and heterogeneous and include the direct activation of extracellular MMP activity (9, 14), activation of MMP gene expression (9, 15, 16) and, finally modulation of MMP mRNA stability as shown for rat MMP-9 (17). In this study we investigated whether in addition to the direct modulation of MMP-9, NO indirectly, by modulating the expression of TIMP-1, affects MMP-9 net activity.

Given the pivotal role of transforming growth factor β (TGFβ) on the deposition of ECM (for reviews see Refs. 18 and 19), we investigated a possible functional role of TGFβ in the NO-dependent modulation of TIMP-1 expression. Most convincingly, the critical role of TGFβ in renal fibrosis is highlighted by studies demonstrating that different TGFβ-antagonizing approaches markedly attenuate ECM accumulation in several models of acute and chronic renal diseases (20–22). Inhibition of TGFβ seems a promising therapeutic strategy for prevention of renal fibrosis, and a variety of strategies antagonizing TGFβ signaling are currently being tested in different clinical trials (for review

* This work was supported by Deutsche Forschungsgemeinschaft Grants EB 257/2-1, PF 361/1-1, PF 361/2-1, and SFB 553. The costs of publication of this article were defrayed in part by the payment of page charges. This article must therefore be hereby marked "*advertisement*" in accordance with 18 U.S.C. Section 1734 solely to indicate this fact.

[1] Both authors contributed equally to this work.

[2] Present address: Dept. of Pharmacology and Toxicology, Faculty of Pharmacy, Al-Azhar University, Cairo, Egypt.

[3] To whom correspondence should be addressed: Pharmazentrum Frankfurt, Klinikum der Johann Wolfgang Goethe-Universität Frankfurt am Main, Theodor-Stern-Kai 7, D-60590 Frankfurt am Main, Germany. Tel.: 49-69-6301-6953; Fax: 49-69-6301-7942; E-mail: w.eberhardt@em.uni-frankfurt.de.

[4] The abbreviations used are: ECM, extracellular matrix; NO, nitric oxide; SBE, Smad-binding element; TGFβ, transforming growth factor β; TIMP, tissue inhibitor of matrix metalloproteinase; EMSA, electrophoretic mobility shift assay; MMPs, matrix metalloproteinases; SNAP, *S*-nitroso-*N*-acetyl-DL-penicillamine; L-NMMA, N^G-monomethyl-L-arginine; MC, mesangial cells; DMEM, Dulbecco's modified Eagle's medium; IL, interleukin; ChIP, chromatin immunoprecipitation; ELISA, enzyme-linked immunosorbent assay; PBS, phosphate-buffered saline.

see Ref. 23). Mechanistically, most of the TGFβ effects on ECM accumulation result from a direct induction of matrix synthesis, but in addition, the simultaneous suppression of ECM-degrading enzymes, most importantly MMPs, may serve to synergistically complement this activity (24). In addition to suppression of MMP gene expression, TGFβ cooperates with other cytokines and growth factors to amplify the expression of TIMP-1 and thereby negatively interferes with MMP activity (25, 26). TGFβ signaling in mammalian cells is mediated through an interaction of type I and type II TGFβ receptors, and both are transmembrane receptors with intrinsic serine/threonine kinase activity. Ligand binding to the high affinity type II receptor results in the recruitment of the type I receptor, which subsequently propagates further signaling to intracellular targets via its receptor kinase activity (27). Therefore, most of the TGFβ-triggered signals comprise a phosphorylation of the receptor-associated signaling devices denoted as Smad proteins, namely Smad-2 and Smad-3 (for reviews see Refs. 28 and 29). Both of these Smad proteins, which are categorized as the "R-Smads" (receptor Smads), upon activation can oligomerize with Smad-4, a member of the "Co-Smad" subfamily, to build up transcriptional active complexes. These complexes subsequently translocate to the nucleus, and by a direct binding to cognate Smad-binding elements (SBEs) regulate the transcription of TGFβ target genes. In this study, we provide a new mechanism by which NO activates the Smad-signaling cascade via a TGFβ-dependent mechanism and thereby amplifies the cytokine-induced expression of TIMP-1.

EXPERIMENTAL PROCEDURES

Materials—Human recombinant IL-1β was from Cell Concept (Umkirch, Germany). Human recombinant TGFβ$_1$ was purchased from Merck/Calbiochem. A neutralizing rabbit pan-specific TGFβ antibody and the Quantikine rat TGFβ$_1$ immunoassay kit were purchased from R & D Systems (Wiesbaden-Nordenstadt, Germany). The NO donors *S*-nitroso-*N*-acetyl-DL-penicillamine (SNAP), DETA-NONOate, and the nitric-oxide synthase inhibitor N^G-monomethyl-L-arginine (L-NMMA) were purchased from Alexis Biochemicals (Grünberg, Germany). The TGFβ-RI kinase inhibitor pyridin-2-yl-4-quinonyl-1*H*-pyrazole was purchased from Merck. 5-Azacytidine was purchased from Sigma. Ribonucleotides, restriction enzymes, and modifying enzymes were purchased from Fermentas (St. Leon-Rot, Germany). Antibodies specifically raised against Ser$^{465/467}$ Smad-2 (antibody 3101) and against total Smad-2 (antibody 3102) were derived from Cell Signaling (Frankfurt am Main, Germany). For supershift experiments, an antibody raised against Smad-2/Smad-3 (antibody 610843) was obtained from BD Biosciences. Antibodies against c-Jun, Smad-3 (sc-8332), Smad-4 (sc-7966), TIMP-1 (sc-5538), as well as control IgG and normal goat serum were obtained from Santa Cruz Biotechnology (Heidelberg, Germany).

Cell Culture—Rat glomerular MC were characterized as described (30) and grown in RPMI 1640 supplemented with 10% fetal calf serum, 2 mM glutamine, 5 ng/ml insulin, 100 units/ml penicillin, and 100 μg/ml streptomycin. Serum-free preincubations were performed in DMEM supplemented with 0.1 mg/ml fatty acid-free bovine serum albumin for 24 h before cytokine treatment. All cell culture media and supplements were purchased from Invitrogen.

Determination of TIMP-1 and TGFβ$_1$ Antigen Levels in Conditioned Media of MC—Levels of TIMP-1 and TGFβ$_1$ antigens in cell culture supernatants were quantified by the Quantikine immunoassay kits from R & D Systems raised against rat TIMP-1 or rat TGFβ$_1$, respectively. Confluent MC ($1.0–1.5 \times 10^6$ cells) on 6-well plates were preincubated in DMEM without fetal calf serum for 24 h and stimulated with or without agents for the indicated times. 20 μl of conditioned media were directly transferred to the microtest strip wells of the ELISA plate. All further procedures were performed following the manufacturer's instructions. The absorbances at 450 nm were measured in a microtest plate spectrophotometer, and antigen levels were determined by appropriate calibration curves.

cDNA Clones and Plasmids—cDNA inserts for rat *MMP-9* and *TIMP-1* genes were generated as described previously (5). A cDNA insert from mouse 18 S rRNA was from Ambion (Austin, TX). A glyceraldehyde-3-phosphate dehydrogenase cDNA clone from rats was generated as described previously (5).

Reporter Plasmids and Transient Transfection of MC—A 0.6-kb promoter fragment from the rat *TIMP-1* gene was cloned by PCR from rat genomic DNA using the gene-specific XbaI-flanked (underlined) forward primer 5′-TCTAGAATATGTGCAGCCACTGCAAAGTTTG-3′, corresponding to a region from nucleotide 866 to 890 of the rat *TIMP-1* gene promoter region (GenBank™, accession number X90486) (31), and the XhoI-flanked (underlined) reverse primer 5′-CTCGAGCTCTAGCGTGTCTCTAGGAGTCCG-3′, corresponding to a region from nucleotide 1523 to 1498 of the rat TIMP-1 promoter. The PCR product was digested with XbaI and XhoI restriction enzymes, cloned into the NheI/XhoI cut "pGL3basic" vector from Promega (Mannheim, Germany), and subsequently sequenced by an automated sequence analyzer ABI 310 (PE Applied Biosystems, Weiterstadt, Germany).

Introduction of a quadruple point mutation into a putative SBE-like binding site (GTCATAGAC to CTTATGGGC) to generate pGL-TIMP-1ΔSBE was performed by using the forward primer 5′-TCCTGGATAACTTATGGGCACTCTCAGTGT-3′ (corresponding to a region from −487 to −457 upstream from the transcriptional start site of the rat *TIMP-1* gene promoter). Generation of a double point mutation into a putative proximal AP-1-binding site (TGAGTAA to GGAGTGA) to generate pGL-TIMP-1ΔAP-1 was performed by using the forward primer 5′-AGTGGGTGGAGGAGTGATGCGTCCAGGAAG-3′ (corresponding to a region from −70 to −41 upstream from the transcriptional start site of the *TIMP-1* gene). All mutant constructs were generated using the QuikChange site-directed mutagenesis kit (Stratagene, La Jolla, CA). The pSBE4-Luc, a cis-reporting pGL3 vector containing four copies of the octameric SBE (GTCTAGAC), was described previously (32). pMBE6-Luc was a corresponding luciferase vector, which instead of the wild type SBE contains three copies of a mutated SBE (GTTTATAC). Both vectors were kindly provided by Dr. Vogelstein (Howard Hughes Medical Institute, Baltimore). Transient transfections of MC were performed using the Effectene reagent (Qiagen, Hilden, Germany) following the manufacturer's instructions. The transfections were done as triplicates and repeated at least three times to ensure reproducibility of the results. Transfection with pRL-CMV coding for *Renilla* luciferase was used to control for transfection efficiencies. Luciferase activities were measured with the dual reporter gene system (Promega, Mannheim, Germany) using an automated chemiluminescence detector (Berthold, Bad Wildbad, Germany).

Northern Blot Analysis—Total cellular RNA was extracted from MC using the TriReagent (Sigma), and RNA was hybridized following standard protocols as described previously (5).

Electrophoretic Mobility Shift Assay (EMSA)—Preparations of nuclear extracts from rat MC and EMSA were performed as described previously (33). Sequences of the double-stranded oligonucleotides used for EMSA were derived from the rat *TIMP-1* gene promoter sequence (GenBank™ accession number X90486) and are depicted in TABLE ONE. Alternatively, consensus Smad SBE oligonucleotides (sc-2603; Santa Cruz Biotechnology) were used for EMSA. DNA-protein complexes were separated from unbound oligonucleotides by electro-

phoresis through native 4.5% polyacrylamide gels and run in 0.5× Tris borate/EDTA.

Competition experiments were done by preincubating the DNA binding reaction for 30 min with different dilutions of a primer stock solution corresponding to 10- (1:100) and 100-fold excess (1:10) unlabeled double-stranded oligonucleotides. The sequences for wild type and mutant (forward) SBE-TIMP-1 oligonucleotides are depicted in TABLE ONE. Supershift analysis was done by preincubation of 1–2 μg of supershift antibody to the binding reaction 30 min prior to the addition of the radioactive labeled oligonucleotides.

TGFβ Neutralization Experiments—The impact of TGFβ on the NO-mediated cell responses was tested by the addition of a neutralizing rabbit pan-specific TGFβ antibody that similarly can neutralize the biological activity of $TGF\beta_1$, $TGF\beta_2$, $TGF\beta_3$, and $TGF\beta_5$. MC were pretreated with 5–10 μg of the neutralizing antibody for 60 min before stimulation. To exclude any unspecific inhibitory effects by the immunoglobulins, cells were treated with the same amount of rabbit IgG instead of the anti-TGFβ antiserum.

Chromatin Immunoprecipitation (ChIP) Assay—ChIP assays of cultured MC were performed by using a ChIP assay kit (Upstate Biotechnology, Inc., Lake Placid, NY). Briefly, 4×10^6 cells on a 10-cm culture dish were stimulated for 4 h and cross-linked for 20 min at 37 °C by the addition of formaldehyde (final concentration 1%). After washing with cold phosphate-buffered saline (PBS), cells were resuspended in SDS lysis buffer supplemented with protease inhibitors and incubated on ice for 10 min. Cell lysates were subsequently sonicated eight times with 20-s bursts in a Branson Sonifier 450 (Branson Ultrasonics, Danbury, CT) to yield input DNA enriched with fragments of ~500 bp in size. 1% (v/v) of the sonicated lysate was immediately heated at 65 °C for 4 h in the presence of 5 M NaCl to reverse cross-links. This DNA was later used for monitoring equal DNA amounts for ChIP ("input DNA"). Sonicated lysates yielded from $\sim 1 \times 10^6$ cells were diluted to 2 ml with ChIP dilution buffer with protease inhibitors. To reduce nonspecific background, lysates were treated with salmon sperm DNA/protein A-agarose beads for 30 min at 4 °C. The precleared lysates were immunoprecipitated with 2.5 μg of antibody specific for either Smad-3, Smad-4, or alternatively with the same amount of control IgG at 4 °C overnight. Immune complexes were collected with salmon sperm DNA/protein A-agarose. After elution of immune complexes, cross-linking was reversed as described above and ethanol-precipitated. Purified ChIP DNA was finally used as a template for PCR. Primers specific for detection of the TIMP-1/SBE region amplifying a region from −511 to −33 of the rat *TIMP-1* gene promoter were as follows: 5′-TCCCAGTTCTGCCACACTCAACT-3′ (sense) and 5′-CCTGGACGCATTACTCATCCACCC-3′(antisense). PCRs were performed with 35 cycles (30 s at 94 °C, 30 s at 52 °C, and 60 s at 72 °C), and PCR products were separated on a 1% agarose gel.

Western Blot Analysis—The total cellular level of Smad-2 and phospho-Smad-2 was analyzed by Western blot analysis in total cellular extracts (50 μg) as described previously (34). Nuclear extracts (20–50 μg) from MC were used for assessing the nuclear import of Smad-4 or c-Jun, respectively. Detection of TIMP-1 from cell supernatants was done by trichloroacetic acid precipitation as described previously (35). To ensure that the supernatants were derived from equal cell numbers, for each experimental condition, cell numbers were determined separately by use of a Neubauer chamber.

Indirect Immunofluorescence Microscopy—To detect nuclear translocation of Smad-4 subconfluent MC were kept serum-free and subsequently treated for 4 h with the indicated reagents. Subsequently, cells were washed with ice-cold PBS and fixed in cold methanol-containing 0.02% (w/v) EDTA and blocked for 30 min in PBS containing 5% (w/v) goat serum. Antibody incubation was done for 1 h and the Smad-4 supershift antibody was used at a dilution of 1:1000. After 1 h antibody incubation, cells were washed several times with PBS and incubated for 30 min with anti-mouse Alexa 488-coupled secondary antibody and thereafter washed again with PBS. Cell nuclei were stained with 4,6-diamidino-2-phenylindole and mounted in Vectashield (Vector Laboratories, Burlingame, CA). Fluorescence was observed immediately with a Zeiss Axioplan upright fluorescence microscope.

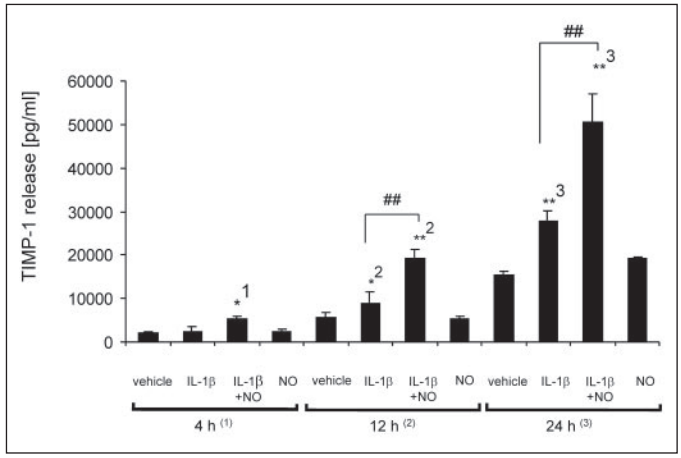

FIGURE 1. **NO potentiates IL-1β-induced TIMP-1 protein levels in conditioned media of MC.** MC were treated with either vehicle, IL-1β (2 nM), SNAP (NO, 500 μM) or both in combination for the indicated times. After stimulation, 20 μl of cell culture supernatants were subjected to Quantikine immunoassay kit for measurement of TIMP-1 protein. Data represent the means ± S.D. ($n = 4$). *, p values <0.05. **, $p \leq 0.01$ compared with vehicle or to IL-1β-stimulated conditions (##) and related to the indicated time point (*number* in *parentheses*).

Methylation-specific PCR Analysis of the 5′-Regulatory Region of the Rat TIMP-1 Gene—Methylation-specific PCR assay was performed as described (36). HpaII (methylation-sensitive) and MspI (methylation-insensitive) restriction enzymes were used to digest genomic DNA from MC treated for 4 h. Briefly, genomic DNA was extracted from MC using the DNAzol reagent (Invitrogen), and 5 μg of DNA was subjected to each digestion reaction with 40 units of vehicle, HpaII, or MspI enzymes, respectively. Subsequently, digested DNAs were purified by standard procedures. 50 ng of digested and not digested DNAs (the latter was used as a negative control) were finally used as a template in PCR amplification with the same primers that were used for the ChIP assay. PCR products were finally resolved on 1% agarose gels.

Statistical Analysis—Results are expressed as means ± S.D. The data are presented as *x*-fold induction compared with untreated vehicle or compared with stimulated values. Statistical analysis was performed using Student's *t* test and analysis of variance test for significance. *p* values <0.05 and <0.01 were considered as significant.

RESULTS

Nitric Oxide Increases the Cytokine-induced Amount of Extracellular TIMP-1—Recently, we have demonstrated that NO potently inhibits the IL-1β-induced expression of MMP-9, which results in a reduction of the gelatinolytic contents within conditioned media of cytokine-treated MC (5). To evaluate whether NO also influences the levels of cytokine-induced TIMP-1 protein, MC were treated with IL-1β in the presence or absence of the NO donor SNAP (500 μM), and cell supernatants were collected after different time points for assessment of extracellular TIMP-1 protein levels. As shown in Fig. 1, treatment of MC with IL-1β (2 nM) caused a gradual and time-dependent increase in the amount of extracellular TIMP-1, which is most obvious at the late time points

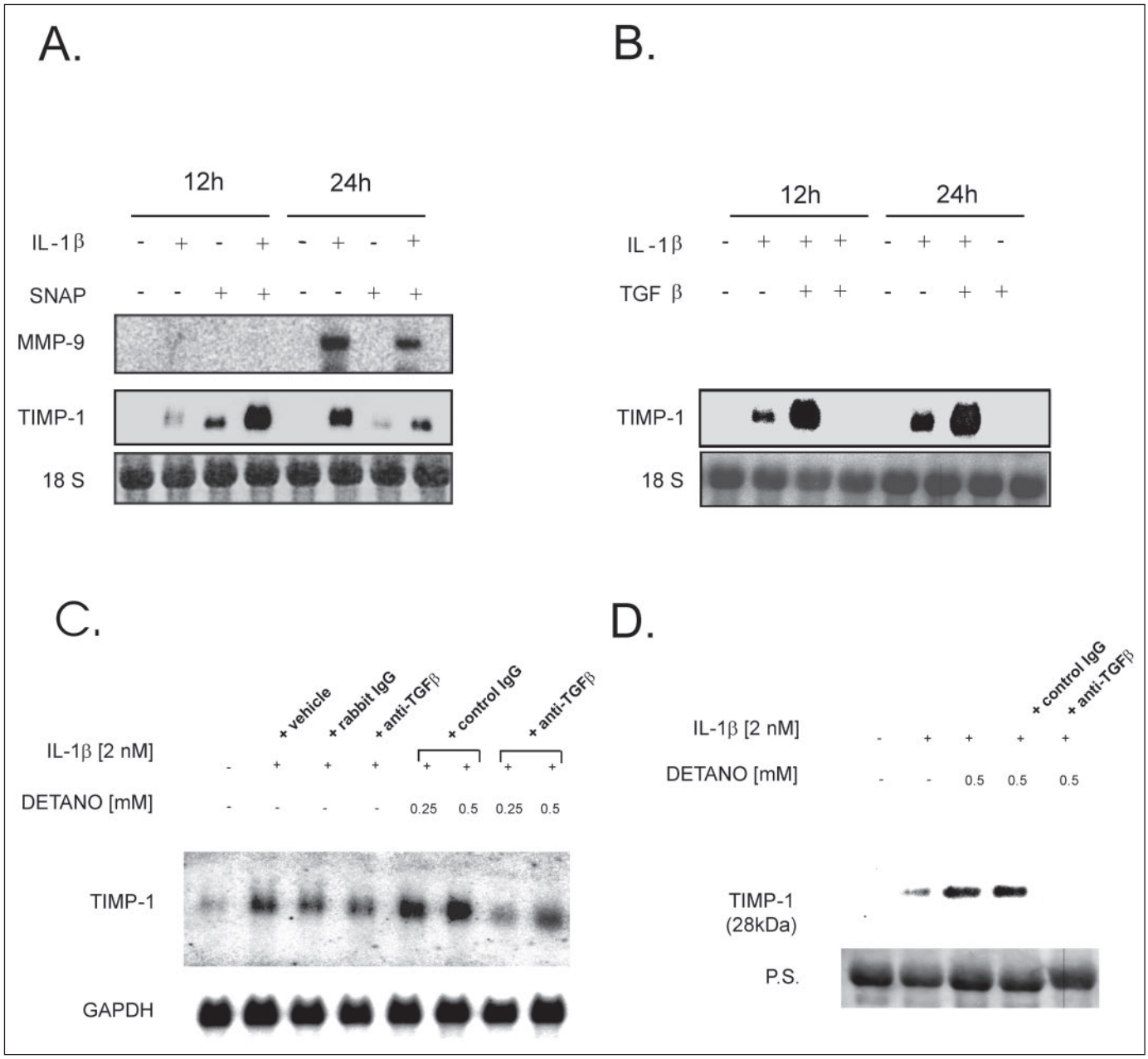

FIGURE 2. *A* and *B*, time-dependent modulation of IL-1β-induced MMP-9 and TIMP-1 steady-state mRNA levels by SNAP (*A*) or TGFβ_1 (*B*). MC were either stimulated with vehicle (−) or with IL-1β (2 nM), SNAP (500 μM), TGFβ (10 ng/ml), or with combinations as indicated for 12 or 24 h, respectively, before total RNA was isolated for Northern blot analysis. Total cellular RNA (20 μg) was successively hybridized to ^{32}P-labeled cDNA inserts from KS-MMP-9 and KS-TIMP-1, respectively. The modulation in mRNA expression by TGFβ_1 was assessed by use of rat-specific TIMP-1 cDNA probe. Equivalent loading of RNA was finally ascertained by rehybridization to an 18 S rRNA probe. Data are representative of two independent experiments giving similar results. The amplification of cytokine-induced TIMP-1 is inhibited by a *Pan*-specific neutralizing TGFβ antibody (*C* and *D*). Quiescent MC were stimulated with the IL-1β (2 nM) with or without the indicated concentrations of DETA-NONOate for 12 h before RNA was isolated for Northern blot analysis (*C*). To test for a possible involvement of TGFβ in the modulation of TIMP-1 expression, MC were additionally pretreated for 60 min in the presence or absence (+*vehicle*) of 10 μg/ml of a *Pan*-specific TGFβ antibody (+*anti-TGFβ*) or isotype-specific IgG (+ *control-IgG*). Equivalent loading of RNA was ascertained by rehybridization to a glyceraldehyde-3-phosphate dehydrogenase (*GAPDH*) probe. *D,* Western blot analysis of trichloroacetic acid-precipitated TIMP-1 in the cell supernatants of MC. For immunodetection of TIMP-1, 0.5 ml of cell supernatant from equal cell numbers was precipitated and subsequently subjected to Western blot analysis using a polyclonal antibody raised against rat TIMP-1. Data are representative of three independent experiments giving similar results. Ponceau-S (*P.S.*) staining of supernatants was performed to control for loading of equal protein amounts.

tested (12 and 24 h). In parallel, the amount of TIMP-1 protein in untreated control cells ("vehicle") slightly increased, which points to a low turnover of extracellular matrix proteins by the endogenous protease/protease inhibitor systems (MMPs/TIMPs) even under serum-free cell culture conditions.

Most interestingly, the addition of SNAP caused a significant increase in the IL-1β-triggered TIMP-1 release that was most prominent after 24 h (Fig. 1). SNAP alone had no significant effects on the basal TIMP-1 levels (Fig. 1). The same effects were observed with the NO donor DETA-NONOate, indicating that the effects on TIMP-1 are specific for NO (data not shown).

Modulation of TIMP-1 by NO Occurs at the Level of mRNA—To test further whether the NO-mediated alterations in the extracellular TIMP-1 levels are preceded by changes in the TIMP-1 mRNA level, we performed Northern blots using a cDNA probe from the rat *TIMP-1* gene. A representative time course experiment is shown in Fig. 2*A*. Most

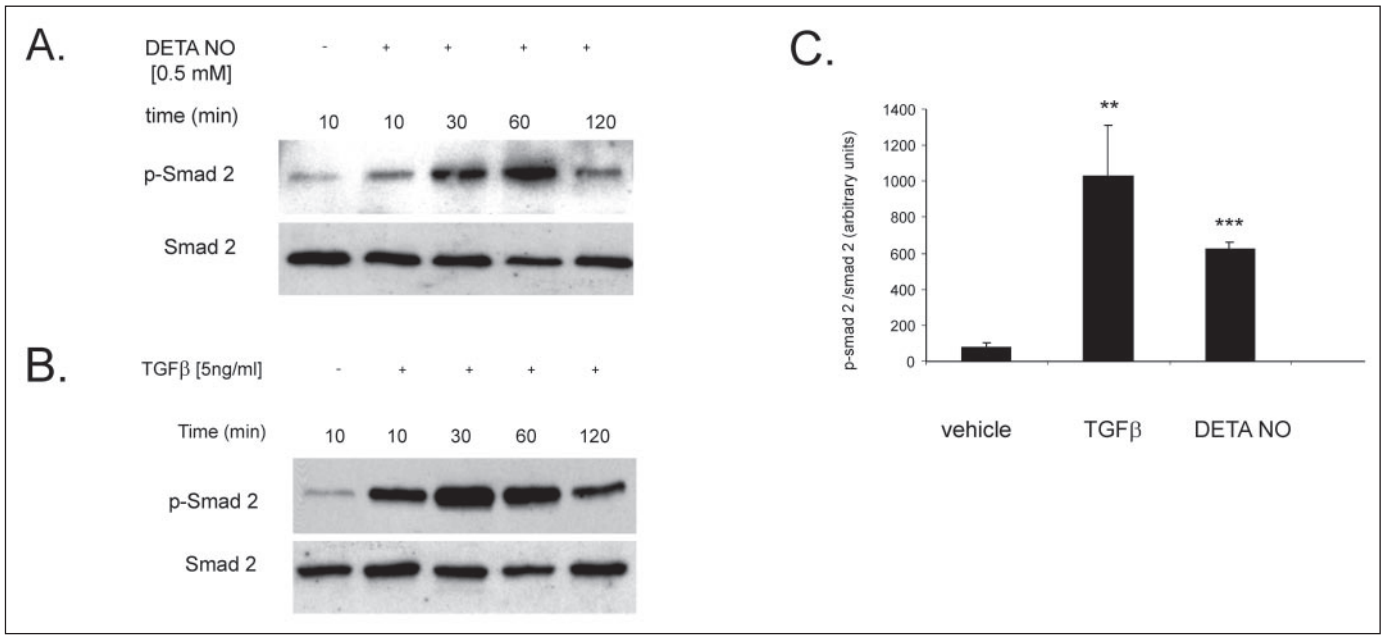

FIGURE 3. *A* and *B*, stimulatory effects of NO (*A*) and TGFβ_1 (*B*) on Smad-2 phosphorylation in MC. Quiescent MC were stimulated with either vehicle (−) or DETA-NONOate (500 μM, *A*) or TGFβ (5 ng/ml, *B*) as indicated for different time points before lysing for Western blot analysis. Total protein (50 μg) was subjected to Western blot analysis and successfully probed with an anti-phospho-Smad-2-specific antibody (*p-Smad 2*) or an antibody raised against total Smad-2 (*Smad 2*). The data are representative for three independent experiments giving similar results. *C*, statistical analysis of phospho-Smad-2 levels after 30 min of stimulation with either DETA-NONOate (500 μM) or TGFβ_1 (5 ng/ml). Data represent means ± S.D. ($n = 3$) **, $p \leq 0.01$.

interestingly, the modulation of IL-1β-induced TIMP-1 mRNA by NO level is biphasic with a strong amplification at the early time point of 12 h and a weak inhibition at 24 h (Fig. 2*A*). More importantly, the effects on basal TIMP-1 steady-state mRNA level by SNAP appeared and also disappeared earlier than the effects exerted by IL-1β (Fig. 2*A*). In contrast to TIMP-1 mRNA, the transcripts of MMP-9, one of the intrinsic targets of TIMP-1, did not appear before 24 h after the addition of IL-1β (Fig. 2*A*). The fact that TIMP-1 expression by inflammatory stimuli precedes MMP-9 expression may guarantee a subtle regulation of protease activity under inflammatory conditions. Similar effects were observed with DETA-NONOate, which again indicates that the changes in TIMP-1 protein levels by NO are independent of the type of NO donor used (data not shown).

Given the early stimulatory effects of IL-1β-induced TIMP-1 mRNA in response to NO, we examined whether TGFβ is involved in the early NO-dependent amplification of cytokine-induced TIMP-1. Besides its pleiotropic role in regulating cell growth and differentiation, TGFβ can induce the expression of matrix protease inhibitors such as plasminogen activator inhibitor-1 (37) and TIMP-1 (38). When testing the modulatory activity of TGFβ_1 on TIMP-1, we found an important similarity with the effects observed for NO. Most interestingly, TGFβ_1 like NO, by exerting only a very weak stimulatory effect on basal TIMP-1 mRNA levels, caused a strong amplification of the cytokine-induced TIMP-1 steady-state mRNA level (Fig. 2*B*). In contrast, TGFβ_1 caused a consistent increase in the cytokine-induced TIMP-1 mRNA levels, thus indicating that the late inhibitory effects of NO are independent from TGFβ.

Neutralization of TGFβ Prevents the NO-mediated Amplification of Cytokine-induced TIMP-1 Levels—A functional involvement of TGFβ in the NO-dependent regulation of TIMP-1 was tested by use of a neutralizing pan-specific TGFβ antibody. This antibody neutralizes the biological activity of TGF-β_1, -β_2, -β_3, and -β_5 (R & D Systems product information). MC were preincubated without (vehicle) or with 10 μg/ml pan-specific TGFβ antibody. Total RNA was isolated after 12 h of stimulation, a time point where the amplification of cytokine-induced TIMP-1 mRNA by NO was most prominent (Fig. 2*A*). As a negative control, isotype-specific IgG was administered instead of the anti-TGFβ antibody (Fig. 2*C*, + *rabbit IgG*). Although the IL-1β-caused increase in TIMP-1 mRNA was only weakly affected by either control IgG or anti-TGFβ antibody, the increase in TIMP-1 mRNA levels caused by cotreatment with cytokine plus DETA-NONOate was strongly abrogated when MC had been preincubated with the neutralizing TGFβ antiserum. In contrast, preincubation with rabbit IgG had no effect on TIMP-1 mRNA level indicating that the inhibitory effects are specifically exerted by the TGFβ-neutralizing antibody (Fig. 2*C*). Corresponding to the inhibition of TIMP-1 mRNA levels, we observed a strong decrease in the extracellular TIMP-1 protein content when MC were pretreated with the pan-specific TGFβ-antibody, whereas incubation with control IgG again did not change the level of TIMP-1 (Fig. 2*D*). These data strongly indicate that the early NO-dependent increase in TIMP-1 expression substantially depends on extracellular TGFβ.

Nitric Oxide Stimulates the Smad Signaling Cascade—To elucidate the molecular mechanism underlying the NO-dependent amplification of cytokine-triggered TIMP-1, we tried to dissect the signaling events triggered by IL-1β from those that are predominantly activated by NO. To this end we first examined whether NO, similar to TGFβ, could induce phosphorylation of Smad-2, a direct target of the activated type I TGFβ receptor (for reviews see Refs. 39 and 40). Stimulation of MC with DETA-NONOate induced a rapid phosphorylation of Smad-2 at Ser^{465} and Ser^{467} that was maximal at 60 min after NO treatment and declined thereafter (Fig. 3*A*). A similar increase in Smad-2 phosphorylation was caused by the NO donor SNAP (data not shown). As a positive control we employed TGFβ_1, a potent activator of Smads. As expected, TGFβ_1 caused a strong increase in Smad-2 phosphorylation, which exceeded the effect of DETA-NONOate (Fig. 3*C*), and maximal levels in phospho-Smad-2 level were already reached after 30 min of stimulation (Fig. 3*B*). In contrast, neither NO nor TGFβ_1 had any effects on the total Smad-2 protein content (Fig. 3, *A* and *B*).

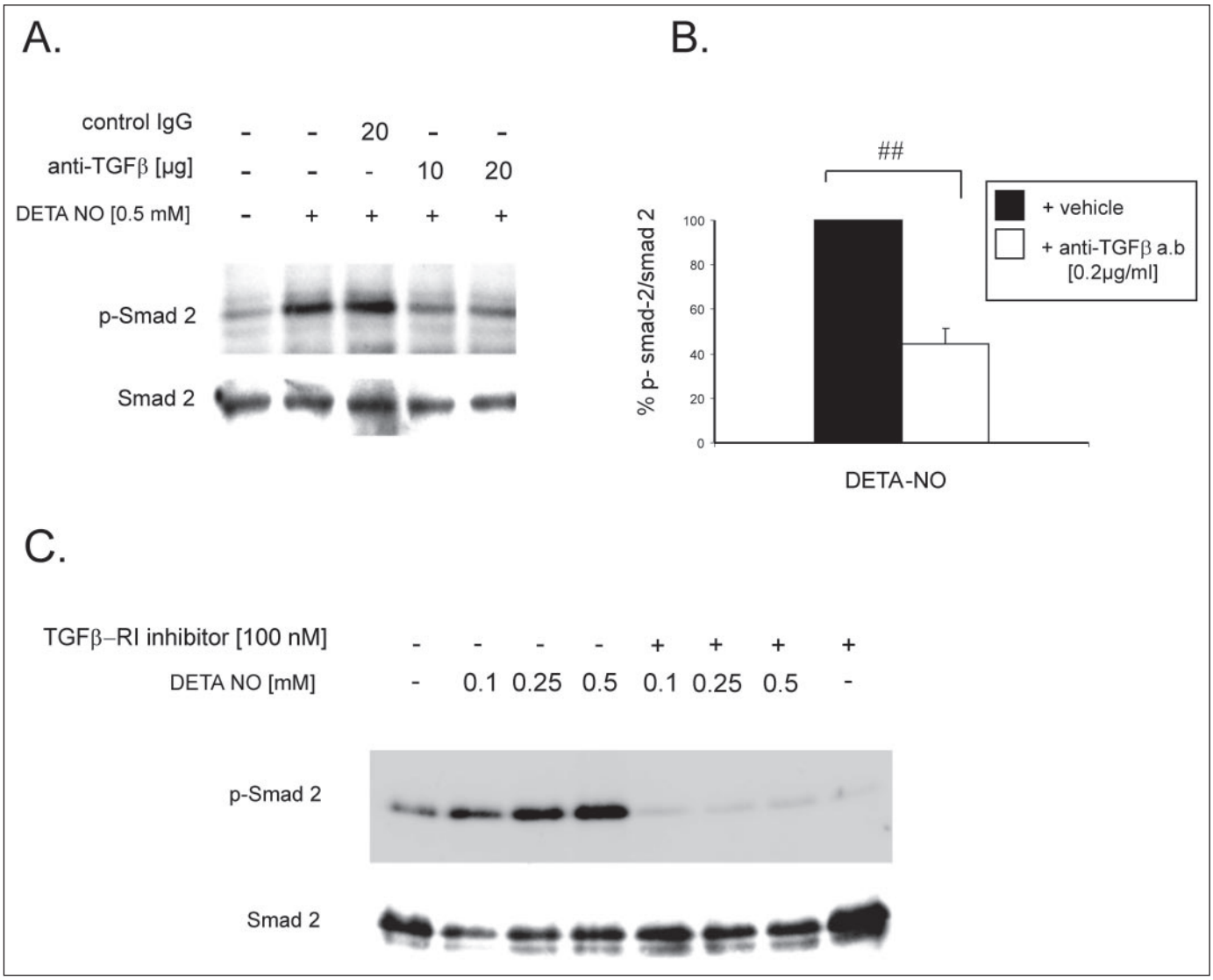

FIGURE 4. **NO-triggered Smad-2 phosphorylation depends on TGFβ and involves TGFβ-RI kinase activity.** *A,* quiescent MC were pretreated for 30 min with or without 20 μg of control IgG as indicated or, alternatively, with the indicated amount of a *Pan*-specific TGFβ antiserum before cells were stimulated for a further 30 min with vehicle (−) or with 0.5 mM DETA-NONOate (+). Thereafter, MC were harvested and Western blots successively probed with anti-phospho-Smad-2 and total Smad-2 antibodies. Data are representative for three independent experiments giving similar results. *B,* densitometric analysis of inhibitory effects of a *Pan*-specific anti-TGFβ antibody (4 μg/ml) on NO-induced Smad-2 phosphorylation. Data represent means ± S.D. ($n = 3$) ##, $p \leq 0.01$. *C,* the dose-dependent increase in Smad-2 phosphorylation by NO is totally blocked in the presence of the specific TGFβ-RI inhibitor pyridin-2-yl-4-quinonyl-1*H*-pyrazole. Quiescent MC were pretreated for 30 min with (+) or without (−) 100 nM pyridin-2-yl-4-quinonyl-1*H*-pyrazole before being stimulated for a further 30 min with the indicated concentrations of DETA-NONOate. Subsequently, cells were harvested and Western blots successively probed with anti-phospho-Smad-2 and total Smad-2-specific antibodies. Data are representative for two independent experiments giving similar results.

The involvement of TGFβ in the NO-triggered Smad-2 activation was also tested by the addition of a neutralizing pan-specific TGFβ antibody. Neutralization of TGFβ caused a significant reduction in NO-induced Smad-2 phosphorylation (60 ± 6% reduction, mean ± S.D., $n = 3$), whereas the addition of isotype-specific control IgG (vehicle) had no effect on Smad-2 activity (Fig. 4, *A* and *B*), thus indicating that the NO-induced increase in Smad-2 phosphorylation depends on extracellular TGFβ.

NO Activates Smad-2 via the TGFβ Type I Receptor—Next we tested whether the stimulatory effects of NO on Smad-2 phosphorylation depend on TGFβ receptor-initiated signaling events. The involvement of the TGFβ-RI in the NO-triggered activation of Smad-2 was tested by use of the specific-TGFβ-RI kinase inhibitor 3-pyridin-4-quinonyl-1*H*-pyrazole, which has demonstrated a high TGFβ-inhibitory potential *in vitro* and *in vivo* (41). Fig. 4*C* shows that incubation with 100 nM of the TGFβ-RI kinase inhibitor totally prevented basal as well as NO-dependent Smad-2 phosphorylation without exerting any inhibitory effects on the total Smad-2 content (Fig. 4*C*).

Endogenously Produced NO Transactivates Smad-2 and Depends on Extracellular TGFβ—Next, we tested whether similar to exogenous NO, endogenous NO secreted by MC after induction of the inducible NO synthase was able to activate Smad-2. Recently, we have demonstrated that the amount of NO produced by induction of the inducible NO synthase expression by IL-1β is in the range that is released by the slow releasing NO donors DETA-NONOate and SNAP (5) and that is necessary to induce Smad-2 phosphorylation (Fig. 3). To this end MC ("recipient MC") were treated for 30 min with the conditioned media collected from MC ("donor cells") treated for 24 h with either vehicle (24 h) or with IL-1β in the presence or absence of L-NMMA (2 mM), a specific inhibitor of NO synthases. Treatment of recipient MC with conditioned medium obtained from untreated donor cells caused only a moderate increase in Smad-2 phosphorylation (Fig. 5*A*), which is most

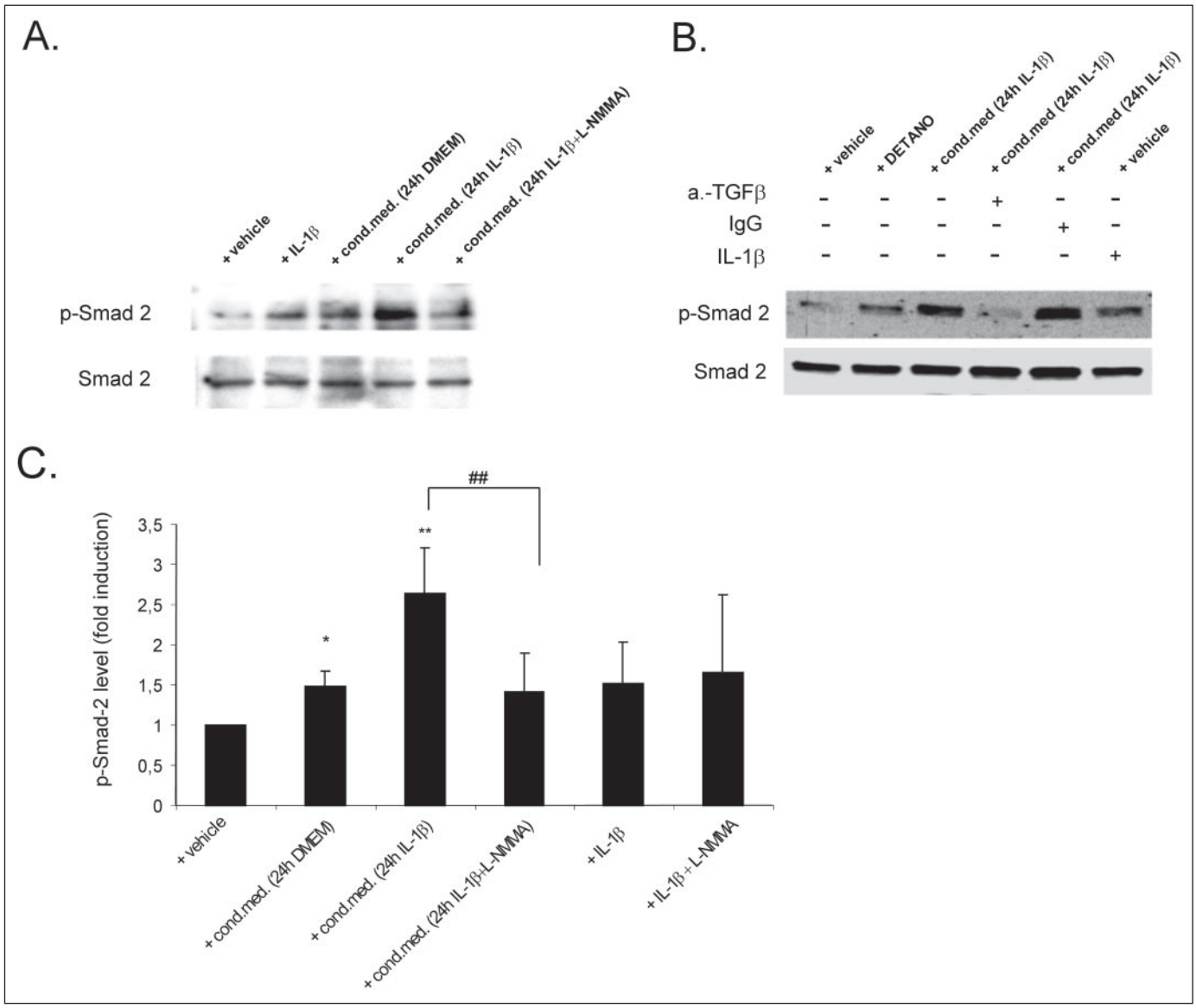

FIGURE 5. **Endogenously produced NO transactivates Smad-2 via TGFβ.** *A,* quiescent MC were treated for 30 min with either vehicle (control) or 2 nM of IL-1β or with the conditioned medium obtained from MC either treated for 24 h with vehicle (+ *cond.med.; 24h DMEM*) or with 2 nM IL-1β in the presence (+ *cond.med.; 24-h IL-1β+L-NMMA*) or absence (+ *cond.med. 24-h IL-1β*) of L-N^G-monomethyl-L-arginine. *B,* alternatively, quiescent MC were treated for 30 min with 0.5 mM DETA-NONOate (+ *DETANO*) or with the conditioned medium obtained from MC treated for 24 h with 2 nM IL-1β (+ *cond.med.; 24 IL-1β*). Before adding the conditioned media to recipient MC, the cell supernatants were either left untreated (−) or incubated for 1 h with 10 μg of control IgG (+) or with 10 μg of a *Pan*-specific neutralizing anti-TGFβ antibody (+). After stimulation, MC were harvested and Western blots successively probed with anti-phospho-Smad-2 and total Smad-2 antibodies. Data are representative for three independent experiments giving similar results. *C,* statistical analysis of three independent experiments demonstrating the stimulatory effects on phospho-Smad-2 levels compared with total Smad-2. Data represent means ± S.D. ($n = 3$). *, $p \leq 0.05$, compared with control (vehicle), or ##, $p \leq 0.01$ compared with the effects exerted by conditioned media from MC stimulated for 24 h with IL-1β (+*cond.med. 24-h IL-1β*).

probably related to the constitutive TGFβ synthesis even during serum-free culture conditions (Fig. 5*A*, + *cond.med. 24h DMEM*),[5] In contrast, a marked increase in Smad-2 phosphorylation was found in MC that were exposed to the conditioned medium from IL-1β-treated donor cells (Fig. 5*A*, + *cond.med. 24-h IL-1β*). Most importantly, a significant reduction in the phospho-Smad-2 level of recipient MC was observed when conditioned medium was derived from cells stimulated with IL-1β but in the presence of L-NMMA (Fig. 5, *A*, and *C*, +*cond.med. 24h IL-1β+L-NMMA*). Again the total Smad-2 content remained unchanged under all conditions (Fig. 5*A*). In contrast, neither IL-1β on its own nor IL-1β in the presence of L-NMMA caused a significant increase in Smad-2 phosphorylation (Fig. 5*C*). Mechanistically, the stimulatory effects of conditioned media from cytokine-treated cells on Smad-2 are mainly attributable to TGFβ because the activation potential of these supernatants was totally abolished by the neutralizing TGFβ antibody but not by control IgG (Fig. 5*B*). The observation that Smad-2 activation caused by conditioned medium from IL-1β-treated donor cells exceeds the Smad-2 phosphorylation in response to DETA-NONOate alone suggests an additional long term stimulatory effect on Smad-2 activity exerted by IL-1β and independent from TGFβ (Fig. 5*B*). In summary, these results demonstrate that the rapid activation of Smad-2 by exogenous NO is partially mimicked by endogenously produced NO via induction of inducible NO synthase (6).

NO Induces Accumulation of Nuclear Smad-4 That Is Paralleled with an Increased DNA Binding to a Cognate SBE—TGFβ signaling via the Smad signal device is further transmitted by a translocation of het-

[5] E.-S. Akool, A. Doller, R. Müller, P. Gutwein, C. Xin, A. Huwiler, J. Pfeilschifter, and W. Eberhardt, unpublished observations.

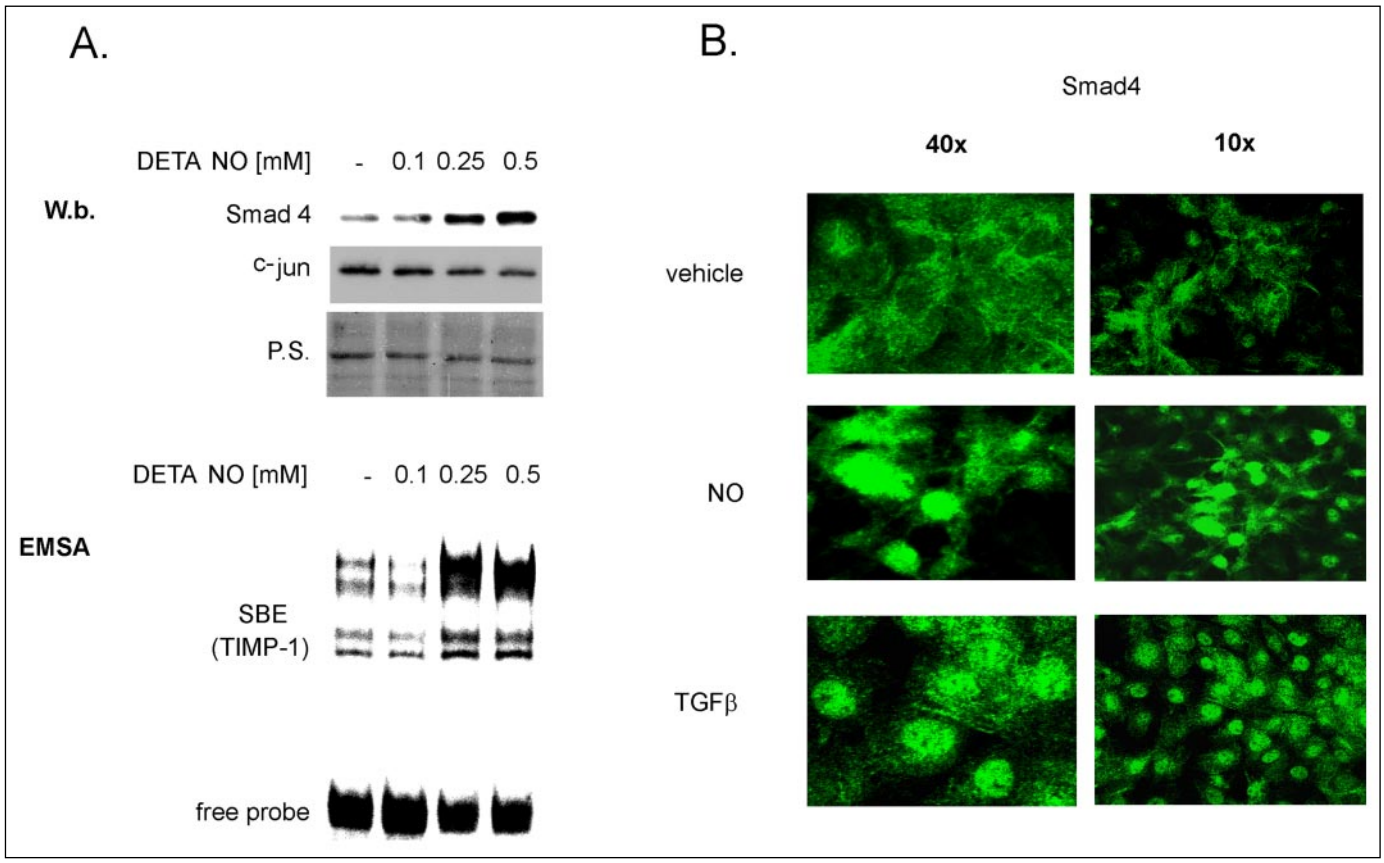

FIGURE 6. **Effects of NO on nuclear Smad-4 and c-Jun contents and on complex formation at a TIMP-1-specific SBE-like promoter element.** Quiescent MC were stimulated for 4 h with vehicle (−) or the indicated concentrations of DETA-NONOate before cells were analyzed by the different approaches. *A, upper panel,* 30 μg of nuclear extracts were subjected to SDS-PAGE and probed with either a Smad-4-specific antibody or an antisera raised against c-Jun. Loading of equal amounts of nuclear extract was ascertained by Ponceau-S staining (*P.S.*) *Lower panel,* 5 μg of the same extracts were subjected to EMSA using ^{32}P-end-labeled oligonucleotides encompassing an SBE-like sequence motif from the rat *TIMP-1* gene (*SBE-TIMP-1*). *W.b.,* Western blot. *B,* indirect immunofluorescence in a ×40 (*left panel*) and ×10 (*right panel*) magnification showing the changes in the localization of Smad-4 after treatment of MC with vehicle, 500 μM DETA-NONOate (*DETANO*), or with 5 ng/ml TGFβ$_1$ (*TGFβ*). After stimulation for 4 h, the cells were fixed and stained with the anti-Smad-4 and anti-mouse Alexa-488 antibodies, respectively. The figure is representative of two independent experiments giving similar results.

TABLE ONE

Oligonucleotides used in EMSA and for generation of mutant TIMP-1 promoter constructs

Consensus binding sites are underlined, and mutations are lowercase italic letters. WT indicates wild type; mut indicates mutant.

Oligonucleotides	Primer sequence (sense)
SBE core (32)	5′-GTCTAGAC-3′
SBE (TIMP-1) WT	5′-TCCTGGATAAGTCATAGACACTCTCAGTGT-3′
SBE (TIMP-1) mut	5′-TCCTGGATAA*c*T*t*AT*g*G*g*CACTCTCAGTGT-3′
SBE consensus WT	5′-AGTATGTCTAGACTGA-3′
SBE consensus mut	5′-AGTAT*catagcgt*TGA-3′
AP-1 (TIMP-1) WT	5′-AGTGGGTGGATGAGTAATGCGTCCAGGAAG-3′
AP-1 (TIMP-1) mut	5′-AGTGGGTGGA*g*GAGT*g*ATGCGTCCAGGAAG-3′

erodimeric complexes containing R- and Co-Smads (Smad-2/Smad-4 or Smad-3/Smad-4) into cell nuclei followed by transcriptional activation of TGFβ target genes (39). To test whether activation of Smad-2 by NO would also result in a nuclear accumulation of Smad-4, we performed Western blot analysis with nuclear extracts using an anti-Smad-4-specific antibody. Treatment of MC with DETA-NONOate caused a dose-dependent increase in nuclear Smad-4 levels (Fig. 6*A*, *upper panel*). The increase in nuclear Smad-4 accumulation was most obvious after 4 h of NO stimulation (data not shown). Similar to DETA-NONOate, TGFβ$_1$ caused a dose-dependent increase in nuclear Smad-4 accumulation, thus indicating that in MC both stimuli can induce Smad-4 translocation to the nucleus (data not shown). In contrast, the low and constitutive levels of nuclear c-Jun, a constituent of the heterodimeric AP-1 transcription factor complex, was not affected by the NO treatment, thus indicating that in rat MC the increase in Smad-4 is not paralleled by an activation of AP-1 (Fig. 6*A*, *upper panel*). Transcriptional activation by Smads in many instances occurs via the direct binding to a cognate SBE (43). Sequence analysis of the rat *TIMP-1* gene promoter identified a sequence motif between position −476 and −467 with a high sequence homology to the palindromic SBE consensus motif, and only one nucleotide insertion is found at position 4 (GTCATAGAC instead of GTCTAGAC) (TABLE ONE). To test the functionality of this putative SBE in the NO-triggered modulation of TIMP-1, we performed EMSA by using a ^{32}P-labeled oligonucleotide

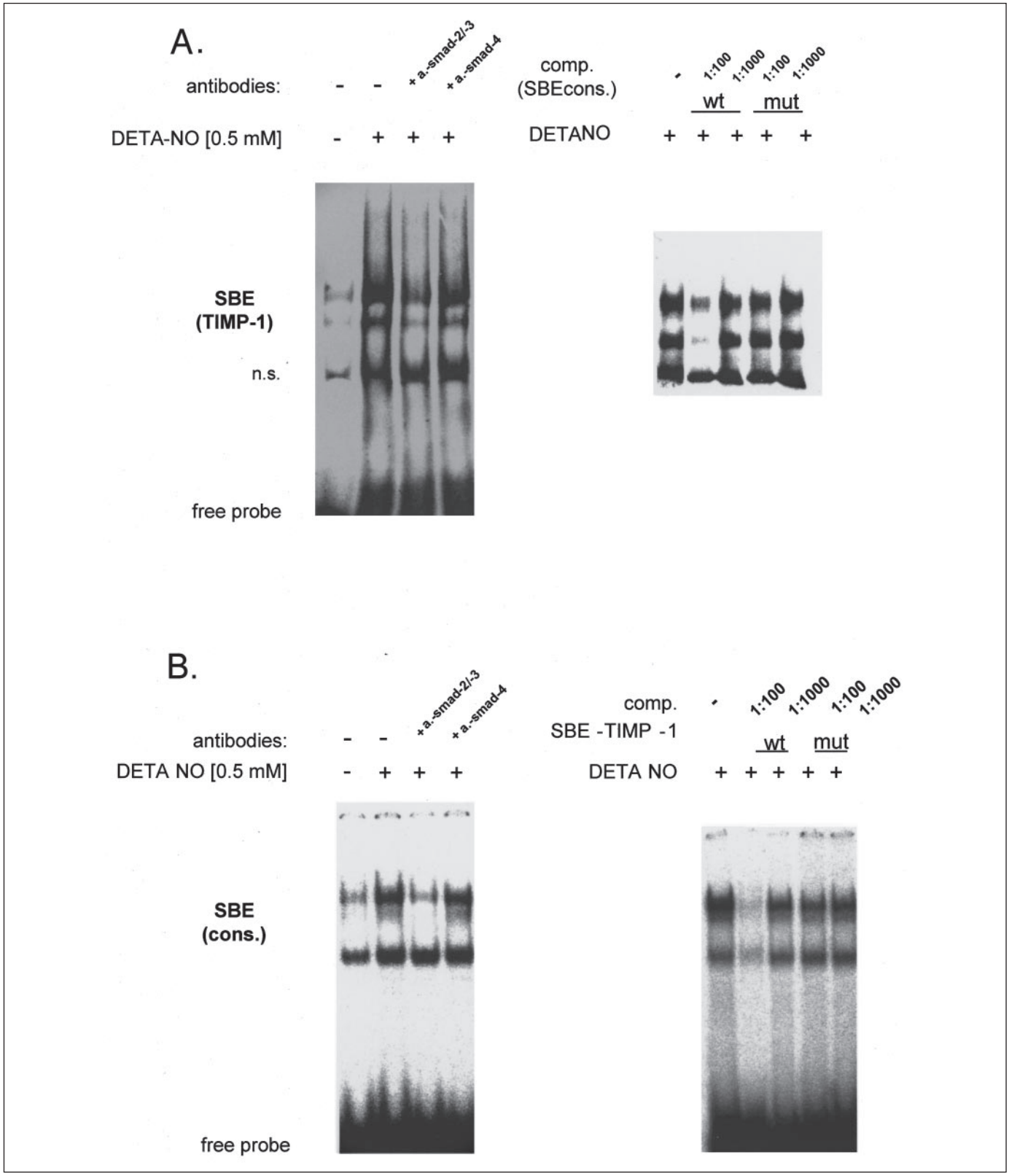

FIGURE 7. **Characterization of NO-inducible complexes binding to the TIMP-1-specific SBE (*A*) or to a consensus Smad-SBE (*B*).** Supershift analysis identifies Smads as the main constituents of NO-induced complexes. Quiescent MC were stimulated for 4 h with vehicle (−) or 0.5 mM DETA-NONOate (+) before cells were lysed for preparation of nuclear extracts. For supershift analysis, anti-Smad-2/Smad-3-specific antibody (+ *a.-Smad-2/-3*) or, alternatively, anti-Smad-4-specific antisera (+ *a.-Smad-4*) were added 30 min prior to the addition of the labeled oligonucleotides. The conditions for DNA binding were as described under "Experimental Procedures." *n.s.*, non-specific. The *right panels* of *A* and *B* show competition capacities of different wild type (*wt*) and mutant (*mut*) SBEs. Different molar excess (depicted as different dilutions of an oligonucleotide stock solution) of the indicated unlabeled competitor oligonucleotide was added 30 min before the addition of the ^{32}P-labeled oligonucleotide. The sequences of the oligonucleotides used for competition experiments are depicted in TABLE ONE. The EMSAs shown are representative of two independent experiments giving similar results.

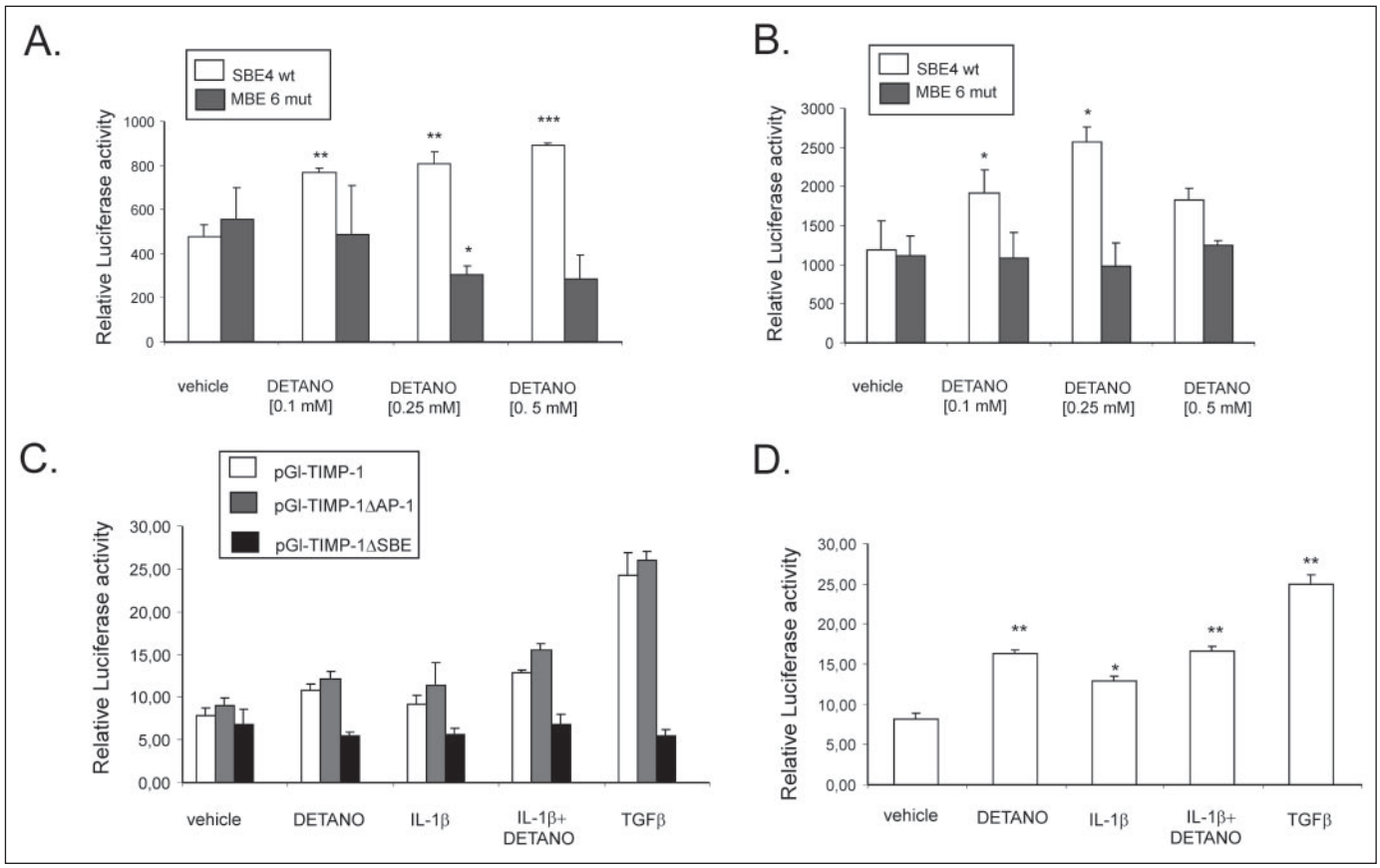

FIGURE 8. **NO stimulates activity of an SBE-driven control promoter.** Subconfluent MC were cotransfected with 0.4 μg of pSBE4-Luc containing four tandem wild type SBEs or, alternatively, with pMBE6mut that containing six point-mutated SBEs and with 0.1 μg of RL-CMV; coding for *Renilla* luciferase was described under "Experimental Procedures." After transient transfection, cells were treated for 12 (*A*) or 24 h (*B*) with the indicated concentrations of DETA-NONOate before assaying for luciferase activities. *C,* alternatively, subconfluent MC were transiently cotransfected with 0.4 μg of either wild type pGL-TIMP-1 (0.6 kb) (*white bars*) or, alternatively, with the same amount of point mutated pGL-TIMP-1ΔAP-1 (*gray bars*) or with pGL-TIMP-1ΔSBE (*black bars*) and with RL-CMV and treated for 12 h with vehicle or with the indicated agents. *D,* subconfluent MC were transiently cotransfected with 0.4 μg of wild type pGL-TIMP-1 (0.6 kb) and with RL-CMV and treated for 24 h with vehicle or with the indicated agents. The values for *beetle* luciferase were related to the values for *Renilla* luciferase and are depicted as relative luciferase activities. Data represent the means ± S.D. ($n = 6$) *, $p \leq 0.05$; **, $p \leq 0.01$, compared with control (vehicle). The agents used for stimulation were used at the following concentrations: DETA-NONOate, 0.5 mM; IL-1β, 2 nM; TGFβ, 5 ng/ml.

comprising the SBE-like motif from the *TIMP-1* gene promoter as depicted in TABLE ONE. Nuclear extracts were prepared from confluent MC either left untreated (−) or stimulated for 4 h with different concentrations of DETA-NONOate (Fig. 6*A*, *lower panel*). Although the nuclear extracts from untreated MC showed a weak constitutive DNA binding of two major complexes, the binding of these complexes was markedly increased upon treatment of cells with 250 and 500 μM DETA-NONOate (Fig. 6*A*). Similar to NO, the treatment of MC with TGFβ_1 clearly increased DNA binding to the SBE-like promoter motif (data not shown).

We also investigated possible NO-mediated changes in the subcellular localization of Smad-4 by indirect immunofluorescence. Under basal conditions we observed that Smad-4 is distributed throughout the whole cell with cytoplasmic staining being much stronger than nuclear staining (Fig. 6*B*, *upper panel*). Treatment of MC with 500 μM DETA-NONOate triggered a substantial accumulation of Smad-4 in the cell nuclei, which was most prominent after 4 h (Fig. 6*B*, *middle panel*). Additionally, we observed a change in the cell shape indicated by retraction of the cell body (Fig. 6*B*, *middle panel*), independent of which the NO donor was used for stimulation (data not shown). Similar to NO, treatment of MC with TGFβ_1 (5 ng/ml) induced a nuclear import of Smad-4-positive signals most prominently seen after 4 h of stimulation (Fig. 6*B, lower panel*).

Characterization of NO-induced Complexes Binding to the SBE-like TIMP-1 Gene Promoter Site—In order to test whether the two complexes assembled to the TIMP-1-specific SBE indeed contain Smad transcription factors, we performed supershift analysis using antibodies specifically raised against a common epitope of Smad-2 and Smad-3 or, alternatively, raised against Smad-4. The addition of the anti-Smad −2/−3 antibody caused a marked reduction in the DNA binding capacity of NO-induced complexes, whereas the anti-Smad-4 antibody caused only a weak reduction in DNA binding (Fig. 7*A*). However, none of the antibodies caused formation of a supershifted band, which indicates that both antisera used for supershift may mask the DNA binding domain of Smad proteins.

The specificity of DNA binding was tested by competition assays. Addition of a high concentration of unlabeled wild type consensus SBE oligonucleotide (1:100) strongly impaired DNA binding, whereas the addition of the same amount of mutated SBE oligonucleotide had almost no effect on DNA binding (Fig. 7*A*, *right panel*). In contrast, none of the oligonucleotides affected the DNA binding capacity when added in a 10-fold higher dilution (1:1000) (Fig. 7*A*, *right panel*).

Accordingly, when we used a probe encompassing an SBE consensus oligonucleotide, the EMSA showed a similar pattern of two constitutively bound complexes, the binding of both complexes being strongly increased upon DETA-NONOate treatment (Fig. 7*B*, *left panel*). Super-

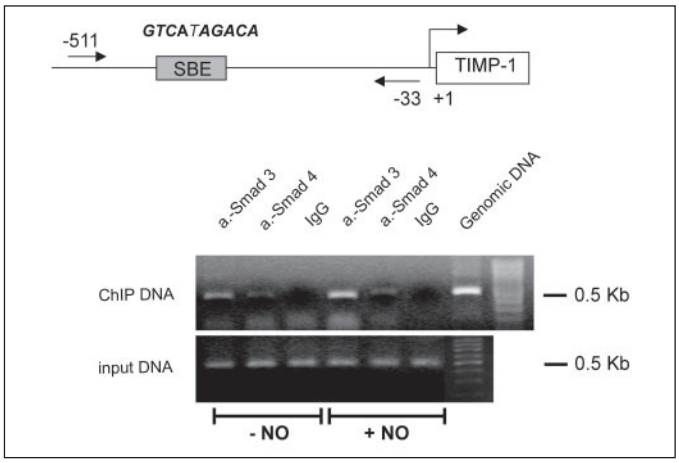

FIGURE 9. **ChIP analysis of Smad-3 and Smad-4 binding to an SBE-like *TIMP-1* gene promoter region.** ChIPs were performed from untreated (−*NO*) and NO-treated (+*NO*) (4 h) MC using antibodies specific for Smad-3, Smad-4, or using rabbit control IgG. The precipitated chromatin was analyzed using primers specific for detection of the TIMP-1/SBE region and amplified a region from −511 to −33 of the rat *TIMP-1* gene promoter encompassing an SBE-like motif (*upper panel*). As a positive control 100 ng of genomic DNA were used as template for PCR (genomic DNA). Input chromatin isolated before the immunoprecipitation was used to control for equal amounts of input DNA (*input DNA*). The experiment shown is representative for two independent experiments giving similar results.

shift analysis revealed that the DNA binding of both NO-regulated complexes was strongly abrogated by the addition of an anti-Smad-2/Smad-3 antibody, whereas addition of an anti-Smad-4 antibody exclusively reduced the DNA binding of the lower migrating complex (Fig. 7*B*, *left panel*). The specificity of the DNA-bound complexes was again corroborated by competition assays. DNA binding was strongly affected by an excess of cold oligonucleotide encompassing the TIMP-1-specific SBE-like motif (1:100), whereas the competition capacity was strongly impaired when a mutated SBE oligonucleotide was used for competition (Fig. 7*B*, *right panel*). These data collectively indicate that NO induces the binding of Smad-2/Smad-3 and Smad-4 containing complexes to a TIMP-1-specific SBE.

The SBE Confers NO-responsive Transcription of TIMP-1—Next, we tested whether NO could also activate a TGFβ-inducible control promoter bearing a tandem of four copies of SBE consensus motifs in front of the luciferase coding region (pSBE4-Luc) (32). Treatment of MC for 12 h caused a significant increase in SBE-driven luciferase activity with all concentrations of DETA-NONOate tested (Fig. 8*A*). Similarly, a significant increase in luciferase activity was observed with all concentrations of DETA-NONOate tested when the treatment of transfected cells was prolonged to 24 h (Fig. 8*B*). Concomitantly, a luciferase reporter gene, which instead of the wild type SBE motifs contained a tandem of six mutated SBE motifs (pMBE6-Luc) (32), was not induced by NO treatment, thus demonstrating that NO-dependent promoter activation is because of cis-activation via an SBE (Fig. 8, *A* and *B*).

Activation of a 0.6-kb TIMP-1 Gene Promoter Fragment by NO, IL-1β, and TGFβ—To evaluate further whether the NO-mediated increase in SBE binding is functionally paralleled by an increase in *TIMP-1* gene promoter activity, we tested for inducibility of a reporter construct containing 0.6 kb of the upstream promoter region of the rat *TIMP-1 gene*. Transient transfection of MC with wild type pGL-TIMP-1 comprising a 0.6-kb promoter fragment was followed by a 12-h treatment with either vehicle, DETA-NONOate (500 μM), IL-1β (2 nM), or both in combination and finally assayed for luciferase activity (Fig. 8*C*, *open bars*). As a positive control, we used TGFβ$_1$ (5 ng/ml). To confirm further a functional role for the SBE-like promoter element, we tested in parallel a corresponding *TIMP-1* gene promoter construct in which the SBE-like core sequence has been point-mutated by an exchange of 4 bp (pGL-TIMP-1ΔSBE) as depicted in TABLE ONE. Furthermore, we tested the impact of a proximal AP-1-binding site, which in some cell types is critically involved in the TGFβ-dependent gene expression (25). A 12-h treatment with NO or with IL-1β shows only a moderate increase in basal luciferase activity, but a 3-fold increase in promoter activity was observed with TGFβ$_1$ (Fig. 8*C*, *open bars*). MC transiently transfected with pGL-TIMP-1ΔAP-1 displayed a similar induction profile in luciferase activity as those derived with the wild type *TIMP-1* gene promoter (Fig. 8*C*, *gray bars*). In contrast, mutation of the SBE-like motif completely impaired promoter induction by NO or by IL-1β (Fig. 8*C*, *black bars*). These data indicate that the SBE-like motif is functionally involved in the promoter induction by NO and TGFβ$_1$, whereas the proximal AP-1-binding site has no impact on the TGFβ-triggered *TIMP-1* gene promoter induction. MC stimulated for 20 h showed an overall stronger increase in *TIMP-1* gene promoter activity than cells that were only stimulated for 12 h (compare Fig. 8, *C* and *D*). The data collectively demonstrate that that TGFβ inducibility of TIMP-1 resides within the 0.6-kb upstream *TIMP-1* gene promoter region. However, the response of this promoter fragment does not reflect the synergistic effects on TIMP-1 mRNA steady-state level by IL-1β in combination with DETA-NONOate (Fig. 8, *C* and *D*), which suggests that additional promoter elements lying upstream from −600 bp are necessary for a synergistic activation TIMP-1 by IL-1β and NO.

Smad-3 and Smad-4 Bind to the TIMP-1 Gene Promoter—Furthermore, interactions of Smads with the *TIMP-1* gene promoter region were assessed by ChIP assays. Antibody-mediated precipitation of fragmented chromatin from formaldehyde cross-linked cell lysates with a subsequent PCR amplification revealed *in vivo* binding of Smad-3 and Smad-4 to a promoter region from −511 to −33 of the rat *TIMP-1* gene (Fig. 9). Most interestingly, the Smad-DNA interaction was not only detected in the chromatin from NO-treated cells but, additionally, in lysates derived from untreated MC (Fig. 9). This confirms the observations made by EMSA, demonstrating a constitutive Smad binding even under basal conditions. The specificity of chromatin binding was shown by the inability of control IgG to yield an appropriate PCR product (Fig. 9).

Analysis of TIMP-1 Gene Methylation in Rat MC—Methylation of CpG islands is an important regulatory mechanism modulating gene expression. Interestingly, NO-induced methylation results in the down-regulation of certain genes (42). Because the *TIMP-1* gene promoter is highly enriched in CpG islands, we tested by methylation-specific PCR whether the NO-dependent effects on TIMP-1 expression involves DNA methylation. This technique makes use of the different sensitivity of the isoschizomeric restriction enzymes HpaII (methylation-sensitive) and MspI (methylation-insensitive) toward methylated DNA (36). A region between −511 and −33 of the rat *TIMP-1* gene contains three adjacent HpaII/MspI recognition motifs (CCGG), and a possible methylation of cytosine in this motif would prevent DNA from digestion by HpaII. We were not able to amplify the PCR target region of TIMP-1 when the DNA has been pretreated with one of these restriction enzymes independent of whether we used genomic DNA from untreated cells or from MC that had been treated with DETA-NONOate (data not shown). The lack of DNA methylation is furthermore affirmed by the fact that addition of 5-azacytidine, an inhibitor of DNA methylation, had no effect on the early NO-dependent amplification of cytokine-induced TIMP-1 mRNA (data not shown).

NO Causes a Rapid Increase in Active TGFβ$_1$—As implicated by the neutralizing effects of the TGFβ antiserum, the modulation of TIMP-1 by NO strongly depends on extracellular TGFβ. To finally assess

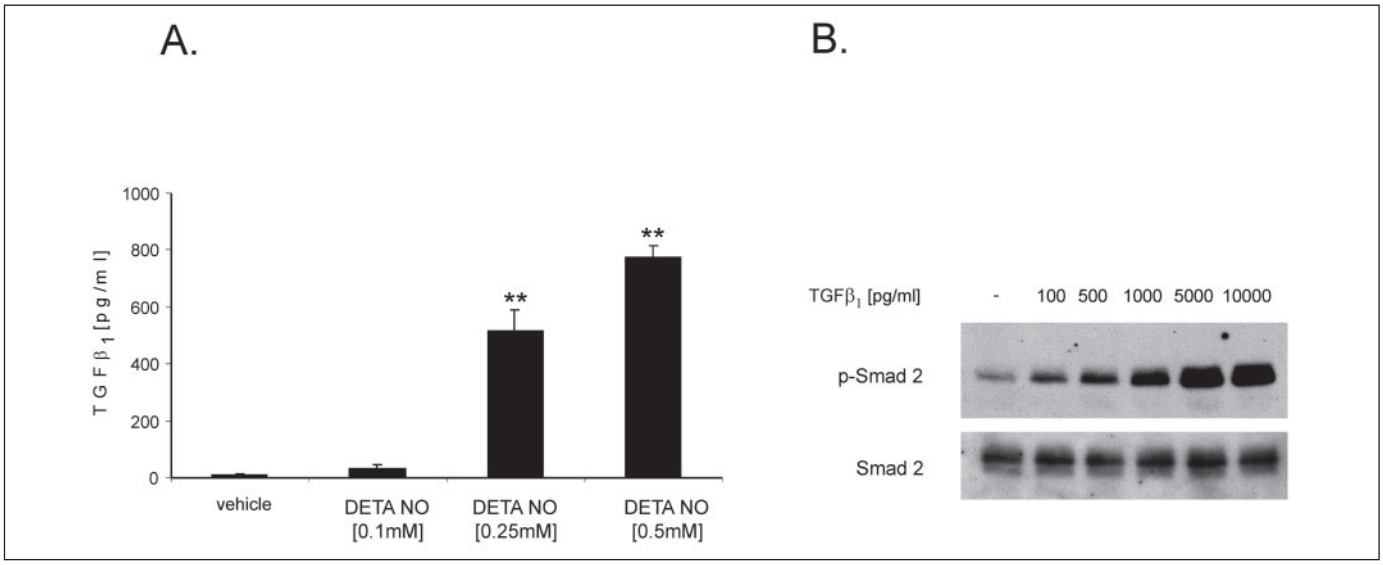

FIGURE 10. **NO dose-dependently modulates active TGFβ_1 secretion by MC (*A*) and subsequent activation of Smad-2 (*B*).** *A,* quiescent MC were treated for 60 min with vehicle or the indicated concentrations of DETA-NONOate before cell supernatants were assessed for active TGFβ_1 by Quantikine ELISA. The omission of a prior acidification of samples allowed the detection of only activated TGFβ_1. Data represent means ± S.D. ($n = 3$). **, $p \leq 0.01$compared with vehicle. *B,* quiescent MC were stimulated with either vehicle (−) or different concentrations of TGFβ as indicated for 60 min before lysing for Western blot analysis. Total protein (50 μg) was subjected to Western blot analysis and successfully probed with an anti-phospho-Smad-2-specific antibody (*p-Smad 2*) or an antibody raised against total Smad-2. The data are representative for two independent experiments giving similar results.

whether NO is involved in the processing of latent TGFβ, we measured the level of active TGFβ_1 within the conditioned media of NO-treated MC by use of a TGFβ_1-specific ELISA. We used an ELISA that is specifically raised against rat TGFβ_1 because commercialized ELISAs against other TGFβ isoforms from rat, to our knowledge, are presently not available. All TGFβ isotypes in most cell types exert similar functions *in vitro* as well as *in vivo,* and most importantly, all TGFβ isoforms equipotently can activate the Smad signaling cascade (44). The detection of the total amount of TGFβ requires activation by acid solutions prior to immunodetection to cleave biologically active TGFβ from latent TGFβ-binding proteins (for review see Ref. 45). The omission of this acidification step allows a detection of active TGFβ. Most interestingly, only concentrations of DETA-NONOate higher than 100 μM caused an increase in the active TGFβ_1 content, and a maximal TGFβ_1 level (~780 pg/ml) was detected after treatment with 0.5 mM DETA-NONOate (Fig. 10*A*).

To further test whether the amounts of endogenously produced active TGFβ_1 levels measured by ELISA are in a range sufficient for activation of the Smad-2, we stimulated MC with different concentrations of recombinant TGFβ1, and we measured Smad-2 activation by use of a phospho-Smad 2-specific antibody. A clear activation of Smad-2 phosphorylation is already seen with the lowest concentration of 0.1 ng/ml TGFβ_1 and maximal Smad-2 phosphorylation seen with a concentration of 5 ng/ml TGFβ (Fig. 10*B*).

These data collectively demonstrate that NO by initiating a rapid increase in active TGFβ can activate the Smad-signaling cascade thereby increasing the cytokine-induced TIMP-1 level.

DISCUSSION

In the present study we provide experimental evidence that NO can activate the Smad-2 signaling cascade, thereby potentiating the cytokine-induced expression of TIMP-1. We furthermore demonstrate that these stimulatory effects, at least partially, can be attributed to activation of latent TGFβ. Because of the central role of TGFβ in the pathogenesis of many fibrotic diseases, these observations suggest that NO at early stages of an inflammatory response display profibrotic properties within the renal mesangium. Physiologically, the occurrence of TIMP-1 preceding that of MMP-9, which is furthermore intensified by NO, may provide a high level of intrinsic MMP inhibitor thus preventing excessive matrix degradation evoked by MMP-9 induction in response to proinflammatory cytokines such as IL-1β and tumor necrosis factor-α. Contrasting to this scenario, the deficiency in ECM degradation is a hallmark of fibrotic processes and in most cases results from a uniform response to the prototypic fibrogenic factor TGFβ (38). Most strikingly, the pathological significance of the TGFβ/Smad pathway in renal fibrosis is highlighted by several experimental studies demonstrating that inhibition of TGFβ by neutralizing approaches could significantly suppress excessive ECM accumulation and thus ameliorate the course of fibrosis (22).

Several studies have demonstrated the antifibrotic properties of the NO pathway in numerous kidney disease models (12, 46–48). Most strikingly, however, several other findings demonstrated that NO, similar to TGFβ, under certain conditions exerts profibrotic properties (11, 12). Collectively, this supports the notion that NO is a multifunctional mediator that can have beneficial as well as deleterious effects in the development of fibrosis, depending on the phase of the disease and the specific model used. In this study, we demonstrate that NO, by rapidly amplifying the cytokine-induced expression of TIMP-1 in MC, may exert an early profibrotic action and thus propagate increased deposition of ECM. We provide evidence that NO by activating TGFβ-dependent signaling cascades can potentiate TIMP-1 expression that is supported by the following findings.

Concomitant with the early potentiation of cytokine-induced TIMP-1 mRNA level by exogenous NO, we observed a significant increase in the extracellular TIMP-1 protein and a similar modulation on TIMP-1 expression was seen with TGFβ. More importantly, the NO-mediated potentiation in TIMP-1 expression is abrogated by a neutralizing, pan-specific TGFβ-antibody without affecting the IL-1β-caused increase in TIMP-1 expression. To the best of our knowledge, we present the first evidence that exogenous NO leads to an activation of the Smad signaling pathway as indicated by a rapid phosphorylation of Smad-2. The velocity of Smad-2 phosphorylation is slightly delayed

when compared with the time course of Smad-2 activation by recombinant TGFβ, which may indicate that NO interferes with the TGFβ signaling cascades further upstream of TGFβ. Most interestingly, the NO-dependent increase in Smad phosphorylation is substantially reduced by a pan-specific TGFβ antibody, further supporting the notion that NO not only mimics TGFβ-mediated Smad activation but also largely depends on extracellular TGFβ. In this regard it is interesting to note that we have recently shown that sphingosine 1-phosphate cross-activates the Smad signaling cascade and thus mimics TGFβ-induced gene expression (34). It still needs to be investigated whether NO, via sphingosine 1-phosphate but independent from TGFβ, is able to activate the Smad signaling cascade.

In line with this we show that the NO-triggered activation of Smad-2 depends on TGFβ-RI kinase activity because incubation with the specific TGFβ-RI kinase inhibitor 3-pyridin-4-quinonyl completely (41) blocked the NO-triggered activation of Smad-2. These inhibitors have demonstrated a high antagonistic potential *in vitro* and *in vivo*, which is several times higher than that observed for other kinases such as the p38 mitogen-activated protein kinase (41). Although both types of TGFβ receptors (TGFβ-RI and TGFβ-RII) display intracellular serine/threonine kinase activities, only the phosphorylated TGFβ-RI does directly target receptor-regulated Smad proteins (R-Smads) (23).

Furthermore, we observed a profound increase in the nuclear Smad-4 level in NO-stimulated MC, thus demonstrating that activation of the Smad cascade by NO also results in an activation of the Co-Smad, Smad-4, which has been identified as a common mediator for almost all Smad pathways (43). A transcriptional induction of TIMP-1 by the NO-mediated Smad activation is furthermore demonstrated by a luciferase construct with a 0.6-kb *TIMP-1* gene promoter fragment that exhibited increased activity upon treatment with NO. This is further corroborated by gel shift assays demonstrating a functional SBE-like promoter sequence within the *TIMP-1* gene that is equipotently activated by NO and TGFβ. This observation is additionally strengthened by the finding that NO, similar to TGFβ, activates expression of an SBE-driven TGFβ-inducible control promoter. The functional importance of an SBE-like motif within the promoter region of the rat *TIMP-1* gene is further indicated by the total loss of NO inducibility observed in pGL-TIMP-1ΔSBE (Fig. 8*C*). Our observations are in line with the previously shown Smad-dependent increase in *TIMP-1* gene promoter activity by TGFβ (38), and the functional importance of Smad-3 for the TGFβ-dependent TIMP-1 expression has been ascertained in fibroblasts from Smad-$3^{-/-}$ mice (49). By contrast, Hall *et al.* (24) reported that TGFβ-triggered TIMP-1 expression is independent of Smad but depends on the AP-1 motif within the *TIMP-1* gene promoter. In addition, heterodimeric Smad/AP-1 containing complexes are involved in the synergistic activation of c-Jun by TGFβ (50).

In contrast to their findings, mutation of an upstream AP-1-binding site had no inhibitory effect on NO inducibility, thus indicating that in rat MC AP-1 does not contribute to the Smad-dependent transcription of TIMP-1. These apparently contrasting findings may be explained by the cell type-specific repertoire of different receptors and Smad-independent pathways that are activated by TGFβ. In this context, it is also worth mentioning that specific inhibitors of the classical extracellular signal-regulated kinase pathway and p38 stress-activated protein kinase cascade do not reduce the NO-dependent increase in Smad-2 phosphorylation, thus indicating that in rat MC the different mitogen-activated protein kinase pathways do not contribute to TGFβ-evoked Smad activation (data not shown).

A main question arises from the obvious inconsistent findings that neither the high basal *TIMP-1* gene promoter activity nor the NO and/or TGFβ-triggered rise in promoter activity is represented by an equivalent increase in the TIMP-1 mRNA levels. Concomitantly, the strong synergistic effects on cytokine-induced TIMP-1 exerted by NO or TGFβ is not reflected by a corresponding amplification in IL-1β-triggered *TIMP-1* gene promoter activity. We suggest that additional promoter elements upstream from −600 are necessary for a full transcriptional response to IL-1β. Additionally, our preliminary results indicate that IL-1β has a positive effect on TIMP-1 mRNA stability, suggesting that IL-1β may inhibit the rapid decay of TIMP-1 mRNA.[5] The elucidation of post-transcriptional TIMP-1 regulation is a further fascinating topic that needs to be addressed by future investigations.

Most intriguingly, we demonstrate that exogenous NO causes a rapid increase in the level of active TGFβ. By contrast, Wang *et al.* (51) have demonstrated that low concentrations of the NO donor DETA-NONOate via the cGMP-dependent protein kinase I suppress the thrombospondin-1-dependent activation of latent TGFβ in response to high glucose in MC. However, the latter study exclusively describes late effects of NO on TGFβ activity occurring after 24 h of stimulation, whereas we have focused on effects that occur after short term incubations (1–16 h). In contrast to the rapid stimulatory effects on Smads reported in this study, the late inhibitory effects on cytokine-induced steady-state TIMP-1 level may as well involve a cGMP-dependent mechanism that is operative in MC and responsible for a NO-mediated inhibition of MMP-9 expression (17). In this context it is important to mention that NO-dependent methylation of CpG islands has been demonstrated as a novel pathway for gene silencing (42). However, Huang *et al.* (36) demonstrated that although its promoter region is enriched in CpG islands, TIMP-1 is not a target of NO-dependent gene silencing. The latter study is in full accordance with our results, although we cannot exclude that the late inhibitory effects on TIMP-1 expression involve NO-dependent methylation of DNA (data not shown).

The majority of cultured cells, including rat MC, have been shown to secrete TGFβ in an inactive form (52, 53). Major physiologic regulators of latent TGFβ activation include different proteases such as MMPs, the serine proteases plasminogen/plasmin, and tissue plasminogen activator but also nonproteolytic proteins such as thrombospondin-1 (53–57). The molecular mechanisms by which NO can interfere with the activation of latent TGFβ as shown here has to be addressed in future investigations. In conclusion, this study demonstrates that NO via TGFβ can amplify cytokine-induced TIMP-1 expression and thereby may play a critical role in the regulation of the proteinase-antiproteinase homeostasis. The molecular mechanisms of the NO-dependent TGFβ activation raise an important topic that, aside from fibrosis, may have implications in the pathogenesis of other TGFβ-triggered diseases, including atherosclerosis and cancer.

Acknowledgment—We thank Dr. Bert Vogelstein (The Johns Hopkins Oncology Center, Baltimore) for sending us the plasmids SBE4-Luc and MBE6-Luc.

REFERENCES

1. Woessner, J. F., Jr. (1991) *FASEB J.* **5,** 2145–2154
2. Nagase, H., and Woessner, J. F., Jr. (1999) *J. Biol. Chem.* **274,** 21491–21494
3. Campbell, C. E., Flenniken, A. M., Skup, D., and Williams, B. R. (1991) *J. Biol. Chem.* **266,** 7199–7206
4. Lotz, M., and Guerne, P. A. (1991) *J. Biol. Chem.* **266,** 2017–2020
5. Eberhardt, W., Beeg, T., Beck, K. F., Walpen, S., Gauer, S., Böhles, H., and Pfeilschifter, J. (2000) *Kidney Int.* **57,** 59–69
6. Pfeilschifter, J., and Schwarzenbach, H. (1990) *FEBS Lett.* **273,** 185–187
7. Pfeilschifter, J. (1994) *News Physiol. Sci.* **9,** 271–276
8. Pfeilschifter, J., Eberhardt, W., and Beck, K. F. (2001) *Pfluegers Arch.* **442,** 479–486
9. Zaragoza, C., Balbin, M., Lopez-Otin, C., and Lamas, S. (2002) *Kidney Int.* **61,** 804–808

10. Eberhardt, W., Beck, K. F., and Pfeilschifter, J. (2002) *Kidney Int.* **61,** 20–30
11. Peters, H., Border, W. A., and Noble, N. A. (1999) *Kidney Int.* **55,** 2264–2273
12. Peters H., Border, W. A., and Noble, N. A. (2000) *Kidney Int.* **57,** 992–1001
13. Pfeilschifter, J., Beck, K. F., Eberhardt, W., and Huwiler, A. (2002) *Kidney Int.* **61,** 809–815
14. Gu, Z., Kaul, M., Yan, B., Kridel, S. J., Cui, J., Strongin, A., Smith, J. W., Liddington, R. C., and Lipton, S. A. (2002) *Science* **297,** 1186–1190
15. Eagleton, M. J., Peterson, D. A., Sullivan, V. V., Roelofs, K. J., Ford, J. A., Stanley, J. C., and Upchurch, G. R., Jr. (2002) *J. Surg. Res.* **104,** 15–21
16. Marcet-Palacios, M., Graham, K., Cass, C., Befus, A. D., Mayers, I., and Radomski, M. W. (2003) *J. Pharmacol. Exp. Ther.* **307,** 429–436
17. Akool, E. S., Kleinert, H., Hamada, F. M. A., Abdelwahab, M. H., Forstermann, U., Pfeilschifter, J., and Eberhardt, W. (2003) *Mol. Cell. Biol.* **23,** 4901–4916
18. Roberts, A. B., McCune, B. K., and Sporn, M. B. (1992) *Kidney Int.* **41,** 557–559
19. Leask, A., Abraham, D. J. (2004) *FASEB J.* **18,** 816–827
20. Ziyadeh, F. N., Hoffman, B. B., Han, D. C., Iglesias-De La Cruz, M. C., Hong, S. W., Isono, M., Chen, S., McGowan, T. A., and Sharma, K. (2000) *Proc. Natl. Acad. Sci. U. S. A.* **97,** 8015–8020
21. Ling, H., Li, X., Jha, S., Wang, W., Karetskaya, L., Pratt, B., and Ledbetter, S. (2003) *J. Am. Soc. Nephrol.* **14,** 377–388
22. Fukasawa, H., Yamamoto, T., Suzuki, H., Togawa, A., Ohashi, N., Fujigaki, Y., Uchida, C., Aoki, M., Hosono, M., Kitagawa, M., and Hishida, A. (2004) *Kidney Int.* **65,** 63–74
23. Yingling, J. M., Blanchard, K. L., and Sawyer, J. S. (2004) *Nat. Rev. Drug Discov.* **3,** 1011–1022
24. Hall, M. C., Young, D. A., Waters, J. G., Rowan, A. D., Chantry, A., Edwards, D. R., and Clark, I. M. (2003) *J. Biol. Chem.* **278,** 10304–10313
25. Edwards, D. R., Murphy, G., Reynolds, J. J., Whitham, S. E., Docherty, A. J., Angel, P., and Heath, J. K. (1987) *EMBO J.* **6,** 1899–1904
26. Leco, K. J., Khokha, R., Pavloff, N., Hawkes, S. P., and Edwards, D. R. (1994) *J. Biol. Chem.* **269,** 9352–9360
27. Lin, H. Y., Wang, X. F., Ng-Eaton, E., Weinberg, R. A., and Lodish, H. F. (1992) *Cell* **68,** 775–785
28. Piek, E., Heldin, C. H., and Ten Dijke, P. (1999) *FASEB J.* **13,** 2105–2124
29. Miyazono, K., ten Dijke, P., and Heldin, C. H. (2000) *Adv. Immunol.* **75,** 115–157
30. Pfeilschifter, J., and Vosbeck, K. (1991) *Biochem. Biophys. Res. Commun.* **175,** 372–379
31. Bugno, M., Graeve, L., Gatsios, P., Koj, A., Heinrich, P. C., Travis, J., and Kordula, T. (1995) *Nucleic Acids Res.* **23,** 5041–5047
32. Zawel, L., Dai, J. L., Buckhaults, P., Zhou, S., Kinzle, R. K. W., Vogelstein, B., and Kern, S. E. (1998) *Mol. Cell* **1,** 611–617
33. Eberhardt, W., Kunz, D., Plüss, C., Hummel, R., and Pfeilschifter, J. (1998) *J. Immunol.* **160,** 4961–4969
34. Xin, C., Ren, S., Kleuser, B., Shabahang, S., Eberhardt, W., Radeke, H., Schafer-Korting, M., Pfeilschifter, J., and Huwiler, A. (2004) *J. Biol. Chem.* **279,** 35255–35262
35. Kämpfer, H., Mühl, H., Manderscheid, M., Kalina, U., Kauschat, D., Pfeilschifter, J., and Frank, S. (2000) *Eur. Cytokine Netw.* **11,** 626–633
36. Huang, X., Orucevic, A., Li, M., and Gorelik, E. (2000) *Clin. Exp. Metastasis* **18,** 329–335
37. Overall, C. M., Wrana, J. L., and Sodek, J. (1989) *J. Biol. Chem.* **264,** 1860–1869
38. Verrecchia, F., Chu, M. L., and Mauviel, A. (2001) *J. Biol. Chem.* **276,** 17058–17062
39. Massague, J. (1998) *Annu. Rev. Biochem.* **67,** 753–791
40. Shi, Y., and Massague, J. (2003) *Cell* **113,** 685–700
41. Sawyer, J. S., Beight, D. W., Britt, K. S., Anderson, B. D., Campbell, R. M., Goodson, T., Jr., Herron, D. K., Li, H. Y., McMillen, W. T., Mort, N., Parsons, S., Smith, E. C., Wagner, J. R., Yan, L., Zhang, F., and Yingling, J. M. (2004) *Bioorg. Med. Chem. Lett.* **14,** 3581–3584
42. Hmadcha, A., Bedoya, F. J., Sobrino, F., and Pintado, E. (1999) *J. Exp. Med.* **190,** 1595–1603
43. Dennler, S., Itoh, S., Vivien, D., ten Dijke, P., Huet, S., and Gauthier, J. M. (1998) *EMBO J.* **17,** 3091–3100
44. Miyazawa, K., Shinozaki, M., Hara, T., Furuya, T., Miyazono, K. (2002) *Genes Cells* **7,** 1191–1204
45. Todorovic, V., Jurukovski, V., Chen, Y., Fontana, L., Dabovic, B., and Rifkin, D. B. (2005) *Int. J. Biochem. Cell Biol.* **37,** 38–41
46. Peters, H., Daig, U., Martini, S., Ruckert, M., Schaper, F., Liefeldt, L., Kramer, S., and Neumayer, H. H. (2003) *Kidney Int.* **64,** 509–518
47. Albrecht, E. W., van Goor, H., Smit-van Oosten, A., and Stegeman, C. A. (2003) *Nitric Oxide* **8,** 53–58
48. Ito, K., Chen, J., Khodadadian, J. J., Seshan, S. V., Eaton, C., Zhao, X., Vaughan, E. D., Jr., Lipkowitz, M., Poppas, D. P., and Felsen, D. (2004) *Kidney Int.* **66,** 1365–1375
49. Ashcroft, G. S., Yang, X., Glick, A. B., Weinstein, M., Letterio, J. L., Mizel, D. E., Anzano, M., Greenwell-Wild, T., Wahl, S. M., Deng, C., and Roberts, A. B. (1999) *Nat. Cell Biol.* **1,** 260–266
50. Wong, C., Rougier-Chapman, E. M., Frederick, J. P., Datto, M. B., Liberati, N. T., Li, J. M., and Wang, X. F. (1999) *Mol. Cell. Biol.* **19,** 1821–1830
51. Wang, S., Shiva, S., Poczatek, M. H., Darley-Usmar, V., and Murphy-Ullrich, J. E. (2002) *J. Biol. Chem.* **277,** 9880–9888
52. Lawrence, D. A. (1996) *Eur. Cytokine Netw.* **7,** 363–374
53. Poczatek, M. H., Hugo, C., Darley-Usmar, V., and Murphy-Ullrich, J. E. (2000) *Am. J. Pathol.* **157,** 1353–1363
54. Schultz-Cherry, S., and Murphy-Ullrich, J. E. (1993) *J. Cell Biol.* **122,** 923–932
55. Munger, J. S., Harpel, J. G., Gleizes, P. E., Mazzieri, R., Nunes, I., and Rifkin, D. B. (1997) *Kidney Int.* **51,** 1376–1382
56. Annes, J. P., Munger, J. S., and Rifkin, D. B. (2003) *J. Cell Sci.* **116,** 217–224
57. Blakytny, R., Ludlow, A., Martin, G. E., Ireland, G., Lund, L. R., Ferguson, M. W., and Brunner, G. (2004) *J. Cell. Physiol.* **199,** 67–76